Characteristics, sources and evolution of fine aerosol (PM$_1$) at urban, coastal and forest background sites in Lithuania

A. Masalaite [a, *], R. Holzinger [b], V. Remeikis [a], T. Röckmann [b], U. Dusek [b, c]

[a] State Research Institute Center for Physical Sciences and Technology, Vilnius, Lithuania
[b] Institute for Marine and Atmospheric Research Utrecht (IMAU), Utrecht University, The Netherlands
[c] Centre for Isotope Research (CIO), University of Groningen, Groningen, The Netherlands

HIGHLIGHTS

- Photochemical processing of organic aerosol at the forest site.
- δ^{13}C of organic aerosol provided insight into sources.

GRAPHICAL ABSTRACT
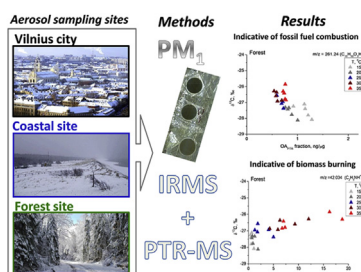
ARTICLE INFO

ABSTRACT

The chemical and isotopic composition of organic aerosol (OA) samples collected on PM$_1$ filters was determined as a function of desorption temperature to investigate the main sources of organic carbon and the effects of photochemical processing on atmospheric aerosol. The filter samples were collected at an urban (54°38′ N, 25°18′ E), coastal (55°55′ N, 21°00′ E) and forest (55°27′ N, 26°00′ E) site in Lithuania in March 2013. They can be interpreted as winter-time samples because the monthly averaged temperature was −4 °C.

The detailed chemical composition of organic compounds was analysed with a thermal desorption PTR-MS. The mass concentration of organic aerosol at the forest site was roughly by a factor of 30 lower than at the urban and coastal site. This fact could be an indication that in this cold month the biogenic secondary organic aerosol (SOA) formation was very low. Moreover, the organic aerosol collected at the forest site was more refractory and contained a larger fraction of heavy molecules with m/z > 200.

The isotopic composition of the aerosol was used to differentiate the two main sources of organic aerosol in winter, i.e. biomass burning (BB) and fossil fuel (FF) combustion. Organic aerosol from biomass burning is enriched in ^{13}C compared to OA from fossil fuel emissions. δ^{13}C$_{OC}$ values of the OA samples showed a positive correlation with the mass fraction of several individual organic compounds. Most of these organic compounds contained nitrogen indicating that organic nitrogen compounds formed during the combustion of biomass may be indicative of BB. Other compounds that showed negative correlations with δ^{13}C$_{OC}$ were possibly indicative of FF. These compounds included heavy hydrocarbons and were on the average less oxidized than the bulk organic carbon.

The correlation of δ^{13}C$_{OC}$ and the O/C ratio was positive at low but negative at high desorption temperatures at the forest site. We propose that this might be due to photochemical processing of OA. This processing can lead to accumulation of carbon in the more refractory organic fraction that is depleted in

---

* Corresponding author.
E-mail address: agne.masalaite@ftmc.lt (A. Masalaite).

^{13}C compared with the less refractory organic fraction. Detailed laboratory experiments are necessary to further investigate the aging of aerosol particles before firm conclusions can be drawn.

1. Introduction

Atmospheric aerosols exert a crucial effect not only on the global but also on the regional climate system (Kaufman et al., 2002; Laj et al., 2009; Monks et al., 2009) as well as on air quality (Dockery et al., 1993; Freney et al., 2014) and human health (Nel, 2005). Air quality monitoring directives usually require the measurement of PM_{10} ($d_p < 10$ μm) and $PM_{2.5}$ ($d_p < 2.5$ μm) concentration levels. However, monitoring of the fine particle fraction ($d_p < 1$ μm) becomes increasingly important as this fraction is the most important to health effects (Pope and Dockery, 2006).

Air quality at different sites (urban, suburban, rural, forest or coastal) depends on various parameters such as local emissions, regional emissions, and transport, as well as on the geographic and meteorological characteristics of the area (Bressi et al., 2014; Freney et al., 2014; Holzinger et al., 2013; Kourtchev et al., 2013; Putaud et al., 2010; Zhang et al., 2015). Several studies analysed contrasting the urban, rural and coastal aerosol concentration and composition in Western Europe (Asmi et al., 2011; Dusek et al., 2013b; Putaud et al., 2004; Weijers and Schaap, 2013), such studies in Eastern Europe are less common (Bovchaliuk et al., 2013; Fountoukis et al., 2014). For this reason we selected three sites in Lithuania, an urban site in Vilnius city (54°38′ N, 25°18′ E), a coastal site at Preila (55°55′ N, 21°00′ E) and a forest location near the village Rugsteliskis (55°27′ N, 26°00' E). A few studies have been carried out previously in Vilnius city (Byčenkienė et al., 2014b; Masalaite et al., 2015; Ovadnevaitė et al., 2006), in Preila (Byčenkienė et al., 2014a; Garbaras et al., 2008; Milukaite et al., 2007; Ulevicius et al., 2010) and at the forest site (Garbaras et al., 2009; Kvietkus et al., 2011; Meinorė et al., 2015). During these studies the input of long range transport to the local aerosol concentration, the relative contribution of organic and elemental carbon, the identification of the pollution sources and characterization of pollution events (biomass burning (BB), summer fires etc.) were explored. Although all these studies yielded valuable information on the physical and chemical characteristics of aerosol particles but they were mostly conducted over short periods of time and/or only at one sampling site at a time. Therefore, there was a clear need to study the origin and the composition of aerosol particles at the same time at all three locations.

The main focus of this study was to gain insight into sources and properties of the organic aerosol fraction by using the detailed chemical and isotopic composition. Organic aerosol (OA) comprises a large percentage of the fine aerosol mass fraction (up to 90%), and their sources, evolution and climate effects are still uncertain (Jimenez et al., 2009). Primary organic aerosol (POA) emitted by fossil fuel combustion (Gelencsér et al., 2007; Masalaite et al., 2015) and biomass burning (Andreae and Merlet, 2001; Ovadnevaitė et al., 2006) is a major fraction of OA. In addition, the secondary organic aerosol (SOA) formed by oxidation of volatile organic compounds (VOC) is also a very important component of OA. OA is often sub-divided into the hydrocarbon–like OA (HOA) that mostly represents the primary organic aerosol that is directly emitted to the atmosphere, and oxidized organic aerosol (OOA), which is dominated by the secondary organic aerosol (Huffman et al., 2009). The application of aerosol mass spectrometer (AMS) measurements combined with factor analysis allows subdividing OOA into two groups based on the mass spectrum derived from aerosol mass spectrometer fragments. One group is associated with less refractory carbon and the other with more refractory carbon, and they are therefore called semi-volatile oxygenated OA (SV–OOA), and low volatility oxygenated OA (LV–OOA) (Holzinger et al., 2013; Presto et al., 2014). These studies indicate that SV-OOA and LV-OOA have different sources and production mechanisms in the atmosphere.

In this study we investigate the composition of organic aerosol desorbed from filter samples at different temperatures using the thermal–desorption proton–transfer–reaction mass spectrometry (TD–PTR–MS) technique (Holzinger et al., 2010b, 2013) that has been described in detail by Timkovsky et al. (2015) and Holzinger (2015). The different desorption temperatures allow an approximate separation of the organic aerosol according to volatility since the less refractory carbon tends to be desorbed at lower temperatures and the more refractory carbon at high temperatures. The PTR-MS is advantageous because of the low detection limits and the capability to detect compounds at their protonated mass (many aerosol compounds do not fragment), which allows detailed characterization of the organic compounds.

The stable carbon isotope ratio of total carbon ($\delta^{13}C_{TC}$) can be used as a tracer to identify and apportion certain pollution sources. For example, aerosol particles derived from marine environments are generally enriched in ^{13}C with δ^{13}C values in the range of −20‰ to −23.3‰ (Ceburnis et al., 2011). Two other sources that can be clearly distinguished are biogenic particles released by C3 plants for which $\delta^{13}C_{TC}$ values vary between −22‰ and −33‰ and particles released by C4 plants with $\delta^{13}C_{TC}$ values between −8 and −18‰ (Deines, 1980). $\delta^{13}C_{TC}$ values of coal combustion derived particles are in the range from −23.4 to −24.4‰ (Widory, 2006). Gasoline/diesel fuel combustion generates particles with $\delta^{13}C_{TC}$ values ranging from −22.6 to −27.2‰ in Western Europe (Widory et al., 2004) and on the average −28 ± 0.9‰ in Eastern Europe (Górka and Jędrysek, 2008; Masalaite et al., 2012, 2015). In Lithuania, aerosol particles emitted from biomass burning had $\delta^{13}C_{TC}$ values varying from −25.5‰ to −27.0‰ (Garbaras et al., 2015), whereas particles of the wildfire origin are very depleted in ^{13}C reaching up to −30.9‰ (Ulevicius et al., 2016; Ulevicius et al., 2010). The most common fuels are spruce pellets $\delta^{13}C_{TC} = -25.8 \pm 0.7$‰ and mixed biomass waste pellets $\delta^{13}C_{TC} = -25.5 \pm 0.5$‰. Therefore, two main sources of aerosol carbon during wintertime (fossil fuel and biomass burning) can be distinguished in Eastern Europe using $\delta^{13}C_{TC}$ (Masalaite et al., 2015).

The carbon isotope ratio can also be a powerful tool to characterise the aging process of OA (Gensch et al., 2014), although not much is known about this process yet (Kirillova et al., 2010). The objective of this work is to better understand the importance of sources of organic carbon (OC) and the isotope effects associated with aging processes in the atmosphere.

2. Methods

2.1. Aerosol sampling sites description

Aerosol sampling was performed from 1 to 29 March 2013 at three sites situated in Lithuania: the urban location of Vilnius (54°

38′ N, 25°, 10′ E), the coastal location of Preila (55° 22′ N, 21°, 1′ E) and the forest location of Rugsteliskis (55° 27′ N, 26°, 0′ E) (Fig. 1). The monthly averaged temperature was −4 °C during the sampling campaign (March of 2013), thus all the samples can be attributed to the wintertime aerosol particles.

The sampling site in Vilnius is close to local pollution sources and therefore represents a typical urban background site. PM_1 size fraction samples were collected daily on workdays (0−24 h) and during Friday−Sunday (0−72 h) on 150 mm diameter quartz microfiber filters (Whatman QM-A) using a high−volume (500 L/min) sampler "Digitel DH−77".

The air pollution monitoring station at Preila is located on the Curonian spit of the Baltic Sea. The nearest industrial city is at a distance of 40 km to the North. A low-volume (30 L/min) aerosol sampler "Leckel" was used to collect samples of PM_1 size fraction on 47 mm diameter quartz filters.

The Rugsteliskis ecological monitoring station is located in a forest in Eastern Lithuania, 30 km from the nearest city to the West. Samples were collected on 75 mm diameter aluminium foils using a high flow (100 L/min) 3-stage impactor "Moudi 128". The impactor has three stages with nominal cut-off of 10, 2.5 and 1 μm. Only the PM_1 size fraction was used for the analysis and data interpretation.

The filters and aluminium foils were heated at 550 °C for 12 h prior to sampling. After sampling, the samples were wrapped in aluminium foil (pre-fired for 12 h at 500 °C), sealed in plastic bags and stored in a freezer (−25 °C) until analysis. One filter blank was collected per week at each site by carrying a filter prepared for measurements to the station and loading it into the sampler for a week without exposing it to the sampling flow.

2.2. $δ^{13}C$ analysis of TC and OC

The $δ^{13}C$ values of bulk total carbon ($δ^{13}C_{TC}$) were determined using one half of a round punch (1.9 mm in diameter) of the quartz fibber filter (or 1/8 of the aluminium foil for a forest site sample). The filter pieces were wrapped into a tin capsule and introduced into an elemental analyser (Flash EA 1112) coupled to an isotope ratio mass spectrometer (Thermo Finnigan Delta Plus Advantage) (EA − IRMS). This method is described in detail in previous studies by Ceburnis et al. (2011) and Garbaras et al. (2008). $δ^{13}C_{OC}$ was measured using a thermal−desorption isotope ratio mass

spectrometry (IRMS) system as described in detail by Dusek et al. (2013a). The system consisted of a quartz glass tube surrounded by two ovens (oven 1 and oven 2), which were coupled to an isotope ratio mass spectrometer. A filter piece was placed into oven 1 at room temperature using a quartz glass filter holder. Both ovens were flushed with helium for another 5 min. The temperature of oven1 was increased starting from 100 °C to 400 °C in steps of 50 °C and at each temperature step organic compounds were desorbed in the helium flow for 7 min. The temperature of oven 2 was kept constant at 550 °C and it was filled with a Platinum catalyst to oxidize the desorbed organic compounds to CO_2. CO_2 was concentrated and purified using two consecutive liquid nitrogen traps and subsequently passed to a gas chromatography column (Varian CP351) to separate CO_2 from possible traces of NO_2 and N_2O. The pure carbon dioxide entered the IRMS via a custom-made open split interface (Röckmann et al., 2003) after water vapour was removed with Nafion dryer.

$δ^{13}C_{TC}$ values measured on the filter samples ($δ^{13}C_{sample}$) were corrected for contamination using the isotope mixing equation. $δ^{13}C_{sample}$ contains contributions from the aerosol collected on the filter and contamination added during the sampling and measurement, which is measured on the blank filters:

$$δ^{13}C_{sample} \cdot ρ_{sample} = δ^{13}C_{aerosol} \cdot (ρ_{sample} - ρ_{blank}) + δ^{13}C_{blank} \cdot ρ_{blank}, \qquad (1)$$

where $δ^{13}C_{blank}$ represents the average $δ^{13}C_{TC}$ value of 3 blank filters collected at each site. $ρ_{blank}$ is the average concentration of TC on the blank filters and $ρ_{sample}$ is the average concentration of TC on the sample filters. The stable carbon isotope ratio of the aerosol $δ^{13}C_{aerosol}$ can be determined from Eq. (1).

The $δ^{13}C_{OC}$ measurement for a given filter was separately corrected using each of the three blank filters according to isotope mixing equation, using respective values for OC at each T step instead of TC. The standard deviation of $δ^{13}C_{OC}$ after blank correction of separate blanks varied from 0.00 to 0.07.

The uncertainty of $δ^{13}C_{TC}$ measurements was estimated as the standard deviation of the $δ^{13}C$ measurements for TC (n = 4). On the other hand, $δ^{13}C_{OC}$ values were usually measured on a single filter piece. However, reproducibility measurements were performed for three different filters, each of which was measured five times. The

Fig. 1. Geographical location of the three sampling sites in Lithuania: Vilnius City, Preila (coastal site) and the remote site in the forest Rugsteliskis.

standard deviation of $\delta^{13}C_{OC}$ averaged over all temperature steps varied between 0.03 and 0.23 for the three filters.

2.3. PTR–MS measurements and data treatment

The offline thermal–desorption proton–transfer–reaction mass spectrometry (TD–PTR–MS) setup (from here on referred to as 'PTR–MS') consisted of an oven system coupled to the PTR–MS which was described in detail by Holzinger et al. (2010b) and Timkovsky et al. (2015).

In short, the oven design was similar to the IRMS system described above. The filter, wrapped into Al foil, was taken out of the freezer and left at the room temperature for 3 min to adjust before the measurement. A filter piece (area of 0.2–4.2 cm^2 depending on the amount of material on the filter) was inserted into the system using a sample holder made from quartz glass. The filter was introduced into the oven and the ovens were flushed with N$_2$ for 2 min to flush out the remaining air and reach stable conditions. The organic compounds were then evaporated from the filters at six temperature steps starting with 100 °C and ending with 350 °C in the step size of 50 °C, lasting for 180 s each. Meanwhile the temperature of oven 2 was kept constant at 200 °C in order to prevent the condensation of the volatilized gasses. The pure nitrogen carrier gas flow was 50 mL/min and it carried the released organic compounds from the first to the second oven, where a fraction of the flow was sampled for the PTR–MS.

The operating conditions of the PTR–MS were as follows. The temperature of the drift tube was 117 °C and the temperature of the inlet line was 180 °C. The pressure in the drift tube was 2.8 mbar and the voltage across the drift tube $U_d = 600$ V and $U_{dx} = 28$ V at the end of the drift tube. The voltage and the current of the ion source were 140 V and 4–5 mA. More than $2.5 \cdot 10^5$ cps (count per second) were detected for the intensity of the primary protonated water ion signal (calculated from the signal at m/z = 21.023). TOF resolution expressed by the mass resolution (defined as Full Width at Half Maximum, FWHM) varied from 3000 to 3500.

The data were evaluated using Interactive Data Language (IDL, version 7.0.0, ITT Visual Information Solutions) with custom-made routines described by (Holzinger, 2015; Holzinger et al., 2010a, 2010b). The unified mass list contained 975 organic compounds identified by their mass to charge ratio (m/z). Initially, the measured concentrations were expressed as volume mixing ratios of the compounds in the N$_2$ carrier gas integrated over the duration of each temperature step (int_VMR), and reported in nmol/mol multiplied by second [s·nmol/mol]. Firstly, the mixing ratio of each individual ion 'i' measured at each temperature step was corrected for the instrument background. The background was defined as the average mixing ratio of ion 'i' measured a few seconds prior to the start of the heating cycle of the oven. Subsequently, a blank correction was performed at each temperature step for each ion. The average mixing ratio of ion 'i' measured on field blank filters was subtracted from the mixing ratio of 'i' measured on each sample. After these corrections the results were converted from the volume mixing ratio in the carrier gas [s·nmol/mol] to ambient concentrations ρ in air [ng/m^3] according to:

$$\rho_i = \frac{J \cdot int\_VMR_i}{V_{air} \cdot S_{piece} / S_{filter}} \cdot MW_i \qquad (2)$$

where J is the flow rate through the oven in units of mol/s, int_VMR is the PTR–MS measured mixing ratio [s·nmol/mol], V_{air} is referred to the volume of the sampled air on a whole filter [in·m^3], S_{piece} [cm^2] is the surface of the measured piece, S_{filter} [cm^2] is the surface of the whole filter, and finally MW_i is the molecular weight of ion 'i'

in units of g/mol.

The individual masses from the mass list were assigned to molecular formulas based on a previously determined mass library (Holzinger et al., 2010a). A detailed description of how molecular formulas are associated with masses from the mass list is given by Timkovsky et al. (2015). Briefly, if more than one formula was possible for a given ion mass, the following rules were used: If the mass was odd, advantage was given to hydrocarbons over oxygenated hydrocarbons. If the mass was even, the first consideration was given to formulas containing nitrogen or carbon-13. However, for formulas with ^{13}C the extra condition that signal$_{m/z}$ < signal$_{(m/z)-1}$*#C*0.022 was applied; where the signal$_{m/z}$ is the signal of the considered ion, the signal$_{(m/z)-1}$ is the signal of the ion with (m/z)-1, #C is the number of carbon atoms in the formula and 0.022 is the factor. The factor 0.022– twice the natural abundance of ^{13}C–ensured that at a certain mass z a formula containing ^{13}C was only attributed if the signal detected at the parent ion of mass z-1 suggested that at least 50% of the measured signal could be attributed to this compound. Finally the formulas with the smallest mass deviation were associated with the ion if several formulas satisfy criteria and were available.

The ions with m/z values below 40 D$_a$ (except for $C_2H_3^+$, CH_2OH^+, CH_5NH^+, and CH_4OH^+, attributed to m/z 27.022, 31.017, 32.049, and 33.034) and m/z values associated with inorganic ions were excluded. Masses 45.99 and 46.00 were related to nitrate and were not considered further. Furthermore, ions that were clearly contaminated (>1000 nmol/mol on the blank) and ions for which the blank accounted for more than 70% of the signal were excluded. A total of 907 ions were left when these rules were applied for data analysis. The total signal of organic aerosol (OA) was the sum of the mass concentration of all 907 organic compounds and will be referred to as OA$_{PTR}$ (in units of ng/m^3 or μg/m^3) in the remainder of the manuscript.

It is worth noting that OA$_{PTR}$ is not the same as organic carbon (OC) measured using a semi-continuous thermal optical carbon analyser (Sunset laboratory) or organic matter (OM) from the aerosol mass spectrometer (AMS) analysis (Takegawa et al., 2005). The oven temperature during filter extraction reached only up to 350 °C, thus the most refractory part of aerosol particles could be left on the filters, whereas the thermal-optical-transmittance method involves evaporation of particles at temperatures up to 650 °C (Cavalli et al., 2010) and the mass concentration of OM, detected using AMS technique, (OM$_{AMS}$) is typically measured at 600 °C (Jayne et al., 2000). Intercomparison of OA$_{AMS}$ and OA$_{PTR}$ shows lower concentrations from PTR–MS (Holzinger et al., 2013) due to loss processes (Holzinger et al., 2010a, 2010b) such as fragmentation of organic compounds during protonation or thermal decomposition during the filter heating in the oven.

The measured ions were divided into five classes according to their chemical formula: hydrocarbons (CH), oxygenated hydrocarbons (CHO), nitrogen containing compounds (CHN), ions containing carbon, hydrogen, oxygen and nitrogen (CHON) and the last group to which no formula could be assigned (unknown). Similarly all the ions were grouped into three classes depending on the m/z ratio. The first group was the sum of all ions up to m/z = 100 (≤100), the second group was the sum of ions from m/z = 100 to m/z = 200 (100–200) and the third group was the sum of ions from m/z = 200 to m/z = 350 (>200).

For the correlation of $\delta^{13}C_{OC}$ with individual ions analysed with the PTR-MS, the mass fraction of each ion at a given temperature step was calculated as the mass of the individual ion (ng) at a given temperature step, divided by OA$_{PTR}$ (μg) at the same temperature step (e.g. C_2H_3NH + mass at 350 °C/OA$_{PTR}$ at 350 °C, (ng/μg)). Scatter plots of the mass fraction vs. $\delta^{13}C_{OC}$ at six temperature steps were analysed for each ion (from m/z = 27 to m/z = 470; 810 ions)

at all three sites. The majority of these ions did not show any correlation with $\delta^{13}C_{OC}$. However, for some ions we found very clear correlations with $\delta^{13}C_{OC}$. Since the mass fractions of the individual ions are too small to significantly influence $\delta^{13}C_{OC}$ directly, we suggest that the respective ions could be indicative of certain aerosol sources or processes.

2.4. PTR–MS and IRMS data comparison

The consistency between PTR–MS and IRMS measurements of the same filters collected in Lithuania in March 2013 at all three sites was evaluated by comparing the PTR–MS analysed organic mass with the IRMS peak area (Fig. 2). The IRMS peaks are assumed over all temperature steps is proportional to the total carbon desorbed from the sample (Dusek et al., 2013a). OA_{PTR} strongly correlated with the IRMS peak area per cubic meter (measured in Vs/m^3) and revealed that the data from both instruments were in good agreement ($r = 0.96$; $p = 1.8 \cdot 10^{-12}$). Since the IRMS peak area is proportional to the amount of carbon (OC) in the sample, this implies that OM/OC ratios are relatively similar for all the samples, which plausible gives the similar chemical composition of the analysed aerosol particles (Fig. 3).

2.5. Additional measurements

Meteorological parameters such as the air temperature, pressure, precipitation, wind speed, wind direction were also collected. Isobaric air mass back trajectories were examined using the National Oceanic and Atmospheric Administration (NOAA) HYSPLIT model (Stein et al., 2015) as one of the aims of the study was to identify regional sources of carbonaceous aerosol. The air mass trajectories were computed for 72 h prior to the sampling at a height of 500 m a.s.l. with a new trajectory starting every 6 h covering the corresponding sampling period.

3. Results

3.1. Chemical composition

The monthly averaged OA_{PTR} was 2.11 $\mu g/m^3$ in the city, 1.11 $\mu g/m^3$ at the coastal and only 0.05 $\mu g/m^3$ at the forest site. However,
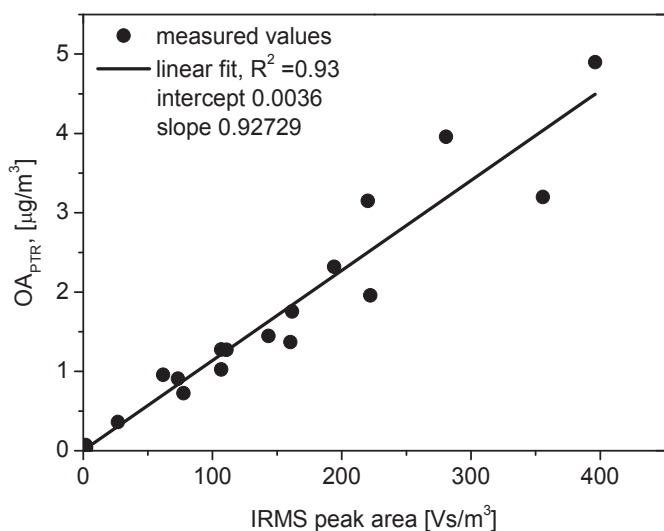
Fig. 2. OA_{PTR} compared with the IRMS peak area (data of aerosol collected in Lithuania in March 2013 at city, coastal and forest sites).
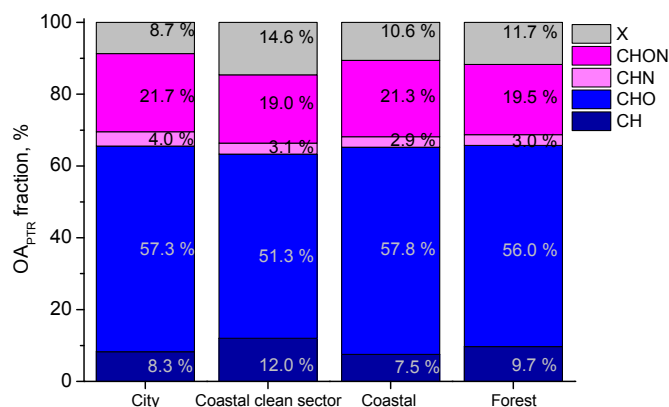
Fig. 3. Percentage of separate ion classes of OA_{PTR} at three sites.

the relative contribution of the five broad chemical classes (CH, CHO, CHN, CHON, and unidentified compounds marked as X) to the analysed organic mass was similar at all three sites (Fig. 3). CHO ions constitute more than a half of OA_{PTR} (1.22, 0.64 and 0.03 $\mu g/m^3$ at the city, coastal and forest sites). The CHON ions accounted for roughly 20% of the analysed organic mass. The fraction of the CH ion mass was similar to the part of the unidentified ions (X) mass (~10%).

The aerosol composition measured in the period of 2–4 March was different from the typical composition at the coastal site (Fig. 3). The air mass back trajectories were from the "clean" sector (Ovadnevaitė et al. (2007)) i.e. the North and the North West during 2–4 March and from "polluted" sectors (Ovadnevaitė et al. (2007)) i.e. the South, the East and the North East during 4–29 March. The data for the coastal site on 2–4 March will be referred to as "Coastal clean sector" and 4–29 March as "Coastal" in the remainder of the manuscript. The hydrocarbons and unidentified ions are enhanced and CHO compounds are reduced in the coastal clean sector samples. This fact is in good agreement with Milukaite et al. (2007), who reported that aerosol in the air from the Northern sector is more associated with the anthropogenic than biogenic origin at this site. OA_{PTR} was 0.36 $\mu g/m^3$ for the costal clean sector only, while for the coastal polluted sector it varied from 0.96 to 1.75 $\mu g/m^3$. The "clean" sector therefore refers to low overall aerosol concentrations, but not to the absence of anthropogenic pollution.

Fig. 4 (a) shows the fraction of OA_{PTR} desorbed at different temperature steps (thermogram) for each site. The highest mass fractions are desorbed at 150 °C for all samples. These thermograms give a rough indication of the refractiveness of the collected OA, even though the desorption temperature from the filter is not a direct measure of the particle volatility. However, thermally less refractory carbonaceous material is usually desorbed at lower temperatures (100–200 °C), whereas the more refractory carbonaceous material tends to be desorbed at higher desorption temperatures (250–350 °C). The mass fraction detected at 100 °C desorption temperature can therefore be considered as typical of the least refractory organic material. A relatively high carbon fraction is desorbed at 100 °C for the urban samples compared to the coastal and forest samples. This implies that the organic aerosol is less refractory in the urban environment in proximity to direct sources. For higher desorption temperatures (250–350 °C) the thermograms at the urban and coastal site are similar. The organic aerosol is overall more refractory at the remote forest site.

Fig. 4 (b) shows a distribution of three different ion groups based on the m/z ratio. Ions with m/z < 100 are categorized as light ions, ions with 100 < m/z < 200 are attributed to the intermediate ions
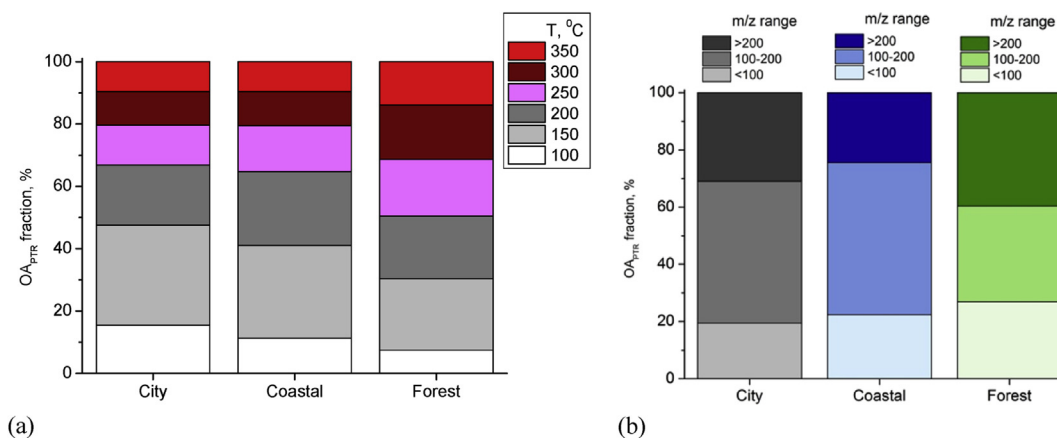
Fig. 4. Thermograms of ambient OA$_{PTR}$ samples collected at city, coastal and forest sites (a) and fraction of OA$_{PTR}$ for three m/z ranges at three sites (b).

and the third group of m/z > 200 represents heavy ions. The light ions (m/z < 100) detected in the PTR-MS do not only represent relatively light organic molecules, but frequently also fragments of larger organic molecules. Fragmentation of organic compounds can occur during thermal desorption in the oven system (Holzinger et al., 2013) or during ionization in the PTR-MS. Fig. 4b shows that OA at the forest site is dominated by heavy ions (40%), whereas OA at the urban and coastal site were dominated by intermediate ions.

OA at the forest site was therefore both more refractory (Fig. 4 (a)) and contained a higher fraction of heavy ions (Fig. 4 (b)) than OA at the other sites. Previous studies (Holzinger et al., 2013; Kroll and Seinfeld, 2008; Timkovsky et al., 2015) showed that photochemical processing produced low volatility compounds and also larger organic compounds (polymeric compounds). The observations at the forest site could therefore be explained by (slow) photochemical aerosol ageing (taking place even in winter) that leads to less refractory material by functionalization.

3.2. Elemental analysis

The van Krevelen diagram (plot of the atomic ratios O/C versus H/C) is often used to investigate compositional differences between complex organic mixtures. The atomic ratio of H/C separates different compounds (ions) according to the degree of saturation, whereas the O/C ratio shows the degree of oxidation. Usually this diagram is plotted for individual compounds or compound classes (HOA, OOA, SV–OOA, LV–OOA etc.), however overall H/C vs. O/C ratios for analysed OA are sometimes presented as well (Chen et al., 2015; Chhabra et al., 2011; Holzinger et al., 2013; Ng et al., 2011; Stubbins et al., 2012). The van Krevelen diagrams for the city, coastal and forest sites are shown in Fig. 5 (a). The O/C ratios for clean sector air masses at the coastal site were lowest, in line with a high fraction of hydrocarbons detected during this period. Overall, the O/C ratios at the three sites varied in a narrow range (from 0.31 to 0.36). The values are in the range reported in the literature for various aerosol sources. An O/C ratio of 0.3–0.38 was reported by Faiola et al. (2015) for biogenic SOA. An O/C ratio of freshly emitted OA from wood burning experiments covered the range of 0.19–0.58 (Widory, 2006). However, the O/C ratio of OA from vehicular emissions is much lower, in the range from 0.022 to 0.15 (Collier et al., 2015). Hallquist et al. (2009) reported that the O/C atomic ratio increases with photochemical processing of the aerosol particles for urban aerosol. The ambient O/C ratios measured in this study could therefore in principle be explained as a mix of different sources.

The second chemical parameter plotted in the Van Krevelen diagram was the H/C ratio. This ratio varied from 1.20 to 1.35, which is generally consistent with the data provided in other studies. Stubbins et al. (2012) reported H/C of dissolved organic matter, the main source of which was anthropogenic aerosol organic matter, varying over a wide range (0.5–2.5). Ng et al. (2011) showed a narrower range (1.1–1.7) of H/C ratios for oxygenated organic aerosol and demonstrated a higher H/C ratio and lower oxidation states for SV-OOA than for LV-OOA components. The narrowest range of H/C for separate SOA elements (1.6 for α-pinene, 0.7–1 for SOA formed from photooxidation of isoprene) was provided by Chhabra et al. (2011), while Faiola et al. (2015) indicated H/C of biogenic SOA to be ~1.5.

A negative slope between the H/C and O/C ratio was observed for the forest site. Such a negative slope is usually taken as an indicator of photochemical aging of aerosol particles (Chhabra et al., 2011; Ng et al., 2011). This negative slope is especially pronounced for the less refractory OA (desorbed at T = 100–200, ^{0}C) (Fig. 5 (b)). Moreover, the more refractory OA (desorbed at T = 250–350, ^{0}C) at the forest site had higher O/C ratios (an indicator of oxidation) than less refractory fraction. These two facts provide evidence that chemical processing (even if it was slow) had influence on the aerosol transported to the forest site. However, the overall H/C ratios of the forest aerosol are higher than for city and coastal aerosol, indicating more saturated aerosol. Therefore, the aerosol at the forest site is probably not simply diluted urban pollution that was transported to the forest site and aged during the transport. It is likely that the aerosol at the forest site has additional sources or is affected by a different mix of sources.

Ten ions with the highest concentrations (out of all detected 907 ions) contributed together 10.9, 14.5 and 11.9% to OA$_{PTR}$ at the city, coastal and forest sites, respectively. The ion at m/z = 97.03 ($C_5H_4O_2H$ + tentatively attributed to be furfural) can originate from biomass burning (Karl et al., 2007; Lewis et al., 2013) and was the main single constituent to the OA$_{PTR}$ at city, coastal and forest sites (Table 1). The m/z = 149.02 ($C_8H_4O_3H+$) ion has been found at high concentrations in a Tunnel study in Brazil (Oyama et al., 2015) and could indicate the influence of traffic pollution. Another important ion m/z = 61.03 ($C_2H_4O_2H+$ – acetic acid/glycoaldehyde) is one of the most abundant organic acids in the ambient atmosphere (Peterson and Richards, 2002). Gas phase acetic acid has been found with PTR–MS measurements earlier, in a study by Holzinger et al. (2007). Andreae et al. (1988) determined that the concentrations of acetic acid in the atmospheric aerosol can be only by 2 orders of magnitude lower than concentrations of the corresponding species in the gas phase. However, in our case acetic acid
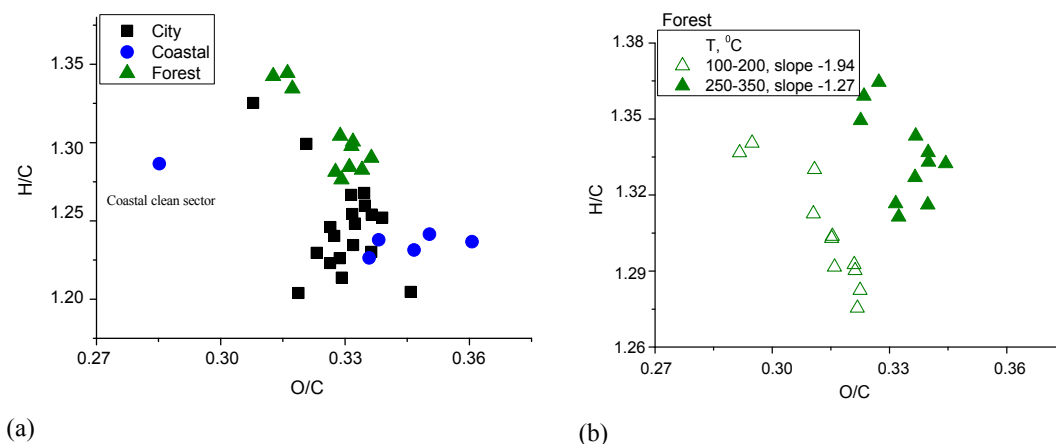
(a)   (b)

Fig. 5. Van Krevelen diagram (plot of the atomic ratios O/C and H/C in OA$_{PTR}$) for city, coastal and forest sites (a) and van Krevelen diagram for organic compounds released in two temperature ranges (100—200 °C; 250—300 °C) for forest data (b).

Table 1
List of 5 ions with the highest relative contribution to OA$_{PTR}$ at the city (orange part of the table), coastal (blue part of the table) and forest sites (green part of the table). **Bolded ions** are the same as ions detected in a tunnel study of diesel vehicle emissions in Brazil (Oyama et al., 2015).

Top range	m/z	formula	Vilnius city (average), ng/m3	% of total organic ions
1	97.03	C5H4O2H+	58.91	2.07
2	**149.02**	**C8H4O3H+**	37.45	1.31
3	61.03	C2H4O2H+	35.52	1.25
4	43.02	C2H2OH+	32.40	1.14
5	**199.04**	**C5H10O8H+**	28.58	1.00
		Sum of 5 ions	192.85	6.77
Top range according to city	m/z	formula	Marine (average), ng/m3	% of total organic ions
1	97.03	C5H4O2H+	45.56	3.39
2	**149.02**	**C8H4O3H+**	25.44	1.90
3	61.03	C2H4O2H+	22.77	1.70
4	43.02	C2H2OH+	18.87	1.41
8	127.04	C6H6O3H+	15.81	1.18
		Sum of 5 ions	128.45	9.57
Top range according to city	m/z	formula	Forest (average), ng/m3	% of total organic ions
1	97.03	C5H4O2H+	1.36	2.53
3	61.03	C2H4O2H+	0.93	1.73
4	43.02	C2H2OH+	0.64	1.20
17	45.03	C2H4OH+	0.64	1.20
7	**203.08**	**C11H10O2N2H+**	0.62	1.15
		Sum of 5 ions	4.19	7.83

is most probably a thermal decomposition product. In conclusion, some of the most important constituents of the organic aerosol can be related to the main OA sources in Lithuania in wintertime, namely biomass burning and fossil fuel combustion.

3.3. Stable carbon isotope composition

$\delta^{13}C_{TC}$ as well as $\delta^{13}C_{OC}$ ratios at different desorption temperatures measured during this study are summarized in Fig. 6. Typical values of $\delta^{13}C_{TC}$ of particles emitted by fossil fuel combustion in

Eastern Europe (−28 ± 0.9‰) (Masalaite et al., 2012 and references therein) are also indicated. These values are consistent with typical $\delta^{13}C$ values of liquid fuels in Eastern Europe (−30.93 ± 0.7‰; Masalaite et al., 2012) combined with a typical fractionation of around −3‰ during fossil fuel combustion (Garbaras et al., 2013; Kawashima and Haneishi, 2012; Widory, 2006). The $\delta^{13}C$ values of most common (commercially available) biomass fuels in Lithuania (Garbaras et al., 2015) are also shown: these are biomass waste pellets ($\delta^{13}C_{TC}$ = −25.1 ± 0.2‰), wood pellets ($\delta^{13}C_{TC}$ = −26.0 ± 0.1‰) and spruce ($\delta^{13}C_{TC}$ = −25.8‰) to a lesser
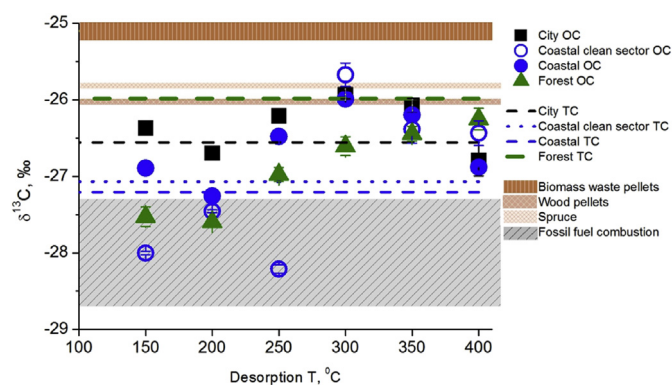
Fig. 6. Comparison of $\delta^{13}C$–thermograms of ambient aerosol samples collected at the city, coastal and forest sites. The solid symbols represent OC desorbed at different temperatures and the dashed and dotted lines represent monthly average values for TC. The range for aerosol from fossil fuel and biomass burning origin based on Masalaite et al. (2015) and Garbaras et al. (2015) are indicated as shading.

extent. Garbaras et al. (2015) found that aerosol emitted from the burning of wood pellets were slightly depleted in ^{13}C compared to the original biomass, i.e., PM_1 $\delta^{13}C$ for biomass waste pellets was $= -25.5‰$ and for wood pellets $-27.0‰$. The $\delta^{13}C$ values of biomass burning aerosol in Lithuania are therefore more variable and less established than the $\delta^{13}C$ values for fossil fuel emissions. However, there is a compelling evidence that carbonaceous aerosol emitted by biomass burning is enriched in ^{13}C compared to aerosol emitted by liquid fossil fuel burning.

Further evidence for two main sources of aerosol particles with different $\delta^{13}C_{TC}$ values comes from an empirical study at Vilnius city during wintertime (Masalaite et al., 2015). In that study the isotope mixing equation was used to test the hypothesis that $\delta^{13}C$ of the ambient aerosol is governed by the mixing of two sources. Only a few pairs of source $\delta^{13}C$ values allowed reproducing the measured isotope values. The obtained value of -28.0 to $-28.1‰$ for source 1 was attributed to fossil fuel combustion and this value was in good agreement with previously reported values of gasoline/diesel fuel combustion generated particles in Eastern Europe ($-28 \pm 0.9‰$) (Masalaite et al., 2012 and the references therein). The second source of aerosol with $\delta^{13}C_{TC}$ value in the range of -25.0 to $-25.5‰$ was named non-fossil source. Garbariene et al. (2016) showed that the continental non-fossil source of carbonaceous aerosol in Lithuania is mainly derived from biomass burning (up to 80%) in wintertime, at least in urban locations. Since the two main OA sources have different $\delta^{13}C$ ratios, variations of $\delta^{13}C_{TC}$ and $\delta^{13}C_{OC}$ ratios of the ambient particles possibly reflect a varying contribution of these sources.

The measured $\delta^{13}C$ values of TC and OC (Fig. 6) were in the range between the reported values of gasoline/diesel fuel combustion generated particles in Eastern Europe and $\delta^{13}C$ values of aerosol particles emitted from biomass burning. $\delta^{13}C_{TC}$ values of aerosol from the coastal site were the most depleted in ^{13}C and $\delta^{13}C_{TC}$ values of particles from the forest site were the most enriched in ^{13}C compared to the average $\delta^{13}C_{TC}$ of all three sites.

$\delta^{13}C_{OC,av}$ was calculated as a mass weighted average of $\delta^{13}C_{OC}$ over all desorption temperatures and subsequently averaged over all samples at a given location. The reported uncertainties correspond to ± 1 standard deviation. On average, the $\delta^{13}C_{TC}$ and $\delta^{13}C_{OC,av}$ values were similar at the city site, suggesting that $\delta^{13}C_{EC}$ (combined with highly refractory OC that is desorbed at temperatures above 350 °C) was similar as well. At the coastal site, the observed $\delta^{13}C_{TC}$ values were slightly lower (but statistically not significant) than $\delta^{13}C_{OC,av}$. Monthly average values for the polluted sector at the

coastal site were $\delta^{13}C_{TC} = -27.3 \pm 0.7‰$ and $\delta^{13}C_{OC,av} = -26.8 \pm 0.6‰$ (p > 0.05). This is consistent with a stronger influence of fossil fuel sources to TC, which can be expected, since EC is usually dominated by fossil sources.

Generally, $\delta^{13}C_{OC}$ at the lowest desorption temperatures was depleted in respect of $\delta^{13}C_{OC,av}$. This is consistent with a larger contribution from FF sources to the less refractory OC. This also corresponds to expectations, since carbon from these sources is generally less refractory than carbon from biomass burning sources. Therefore, fossil fuel sources will influence $\delta^{13}C_{OC}$ more strongly at the lowest desorption temperatures. This is especially pronounced for the coastal clean sector where $\delta^{13}C_{OC}$ varied most strongly with desorption temperature from around $-28‰$ at the T = 150−250 °C to around $-26‰$ at the higher desorption temperatures.

The difference in the carbon isotopic composition between TC and OC was larger at the forest site than at the other sites (Fig. 6) with higher $\delta^{13}C$ values for TC than for OC. The $\delta^{13}C_{TC}$ monthly average value of samples collected at the forest site was of $-26.0 \pm 0.5‰$, whereas the monthly average for $\delta^{13}C_{OC,av}$ was $-26.9 \pm 0.2‰$. The difference was statistically significant at the 95% confidence level (p = 0.004). $\delta^{13}C_{OC,av}$ is similar to the $\delta^{13}C$ values of benzene and toluene reported by Saccon et al. (2015).

The reason for this difference is not entirely clear. The minimum $\delta^{13}C$ value of OC was observed at 200 °C temperature and the highest value at 400 °C. It is possible that OC that desorbs at T > 400 °C would be even more enriched than the $\delta^{13}C$ values measured at lower desorption temperatures. In this case the $\delta^{13}C$ values for the carbon being desorbed at T < 400 °C might not be representative for the total OC. On the other hand, it is also possible that at the forest site there might be an additional OC source that is depleted in respect of $\delta^{13}C_{TC}$. Such a source could be for example SOA formation from terpenes (Fisseha et al., 2009) or α-pinene (Meusinger et al., 2016) that takes place to a small extent even in winter. Since aerosol concentrations at this site were very low, this small amount could have left an isotope signature in $\delta^{13}C_{OC}$. Moreover, the contribution of SOA might explain why O/C at the forest site is in the range of that at the city and coastal site, even though there is evidence of aging, which should have increased the O/C ratio.

3.4. Aerosol sources and chemical processing

The correlation of $\delta^{13}C_{OC}$ with the mass fraction of individual ions can be helpful to investigate aerosol sources and chemical processing. The mass fraction of individual ions was calculated as the mass concentration of the individual ion/total organic mass analysed at a particular temperature step.

Since fossil fuel sources in Lithuania are depleted in ^{13}C compared to other sources (non-fossil), a negative slope of $\delta^{13}C_{OC}$ versus the mass fraction of a certain ion suggests that the molecule in question is related to fossil fuel emissions. These ions will be referred to as "indicative of FF" in the remainder of the manuscript. Examples of such indications are m/z = 261.24, $C_{15}H_{32}O_3H^+$ ion (r = −0.71; p = $8 \cdot 10^{-5}$) at the forest site (Fig. 7 (a)) and m/z = 121.10, $C_9H_{12}H^+$ ion (r = −0.45; p = $6 \cdot 10^{-4}$) at the city site (Fig. 7 (b)) that were negatively correlated over all the temperature range. A significant negative slope was found for 27 ions at the forest site, 6 ions at the coastal site and only 4 ions at the city site (Table 2). Most of the ions we classify as indicative of FF belong to the CHO class (1 at city site, 5 at coastal and 18 at forest site). 19 ions (out of 24) contained from one to four oxygen atoms in these CHO compounds, thus the compounds exhibiting a negative correlation with $\delta^{13}C_{OC}$ are on average less oxidized than the bulk OC. High molecular weight CH ions with the number of carbon atoms
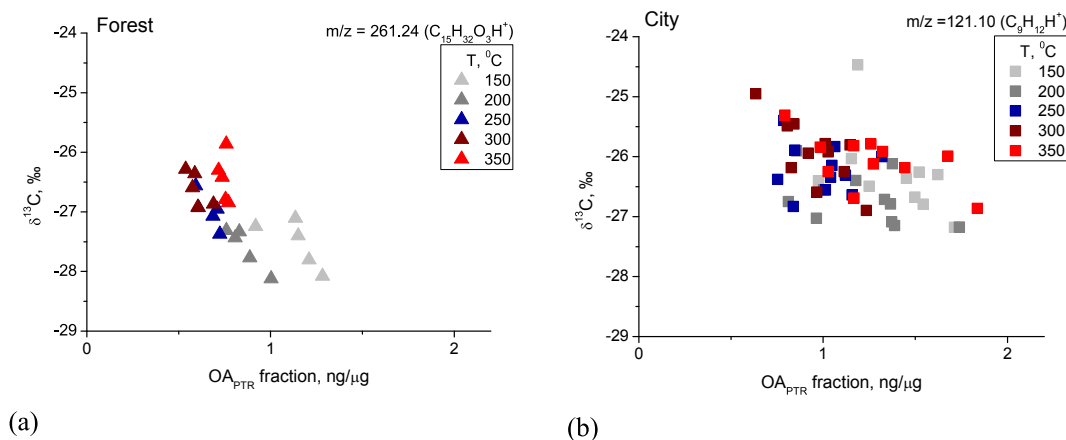
Fig. 7. OA_{PTR} fraction via $\delta^{13}C_{OC}$ values for individual ions as indicative of FF combustion at forest (a) and city (b) sites and the CH, % from all OA_{PTR} fraction via $\delta^{13}C_{OC}$ values at forest (c) and city (d) sites.

Table 2
Two groups of indicative of pollution sources. The table presents the number of ions that undoubtedly ($p < 0.05$) are indicative of FF or BB at each site, enumeration of ions (m/z values) and tentatively attributed formula in the brackets. Indicative of BB was characterized by positive correlation and high concentrations at the high desorption temperatures. Indicative of FF was distinguished by high concentrations in low (or all) temperature intervals and/or a negative correlation in the low (or all) temperature intervals. **Bolded ions** are the same as ions detected in a tunnel study of diesel vehicle emissions in Brazil (Oyama et al., 2015).

Indicative of FF		Indicative of BB
4 ions at city site:		**12 ions at city site**
109.10 ($C_8H_{12}H^+$),		33.03 (CH_4OH^+)
121.10 ($C_9H_{12}H^+$),		42.03 ($C_2H_3NH^+$)
123.11(X),		44.01 (X)
153.09 ($C_9H_{12}O_2H^+$)		54.03 ($C_3H_3NH^+$)
6 ions at coastal site:		56.05 ($C_3H_5NH^+$)
273.24 ($C_{16}H_{32}O_3H^+$),		58.03 ($C_2H_3ONH^+$),
287.27 ($C_{17}H_{34}O_3H^+$),		76.04 ($C_2H_5O_2NH^+$),
301.21 ($C_{20}H_{28}O_2H^+$),		80.01 (C_4HONH^+),
302.21 ($^{13}CC_{19}H_{28}O_2H^+$),		104.4 ($C_7H_5NH^+$),
313.30 ($C_{23}H_{36}H^+$),		120.04 ($C_7H_5ONH^+$),
339.33 ($C_22H_{42}O_2H^+$)		124.99 (X),
27 ions at forest site:		136.04 ($C_7H_5O_2NH^+$)
47.06 ($CH_6N_2H^+$),	276.11 ($C_{11}H_{17}O_7NH^+$),	**2 ions at coastal site:**
89.94 (X),	279.16 ($C_{16}H_{22}O_4H^+$),	114.02 (X),
99.01 ($C_4H_2O_3H^+$),	279.18 ($C_{20}H_{22}OH^+$),	199.04 ($C_5H_{10}O_8H^+$)
99.04 ($C_5H_6O_2H^+$),	287.27 ($C_{17}H_{34}O_3H^+$),	**9 ions at forest site:**
99.08 (X),	289.28 ($C_{17}H_{36}O_3H^+$),	42.03 ($C_2H_3NH^+$),
127.07 ($C_7H_{10}O_2H^+$),	317.40 (X);	54.03 ($C_3H_3NH^+$),
181.07 ($C_6H_{12}O_6H^+$),	323.11 ($C_{16}H_{18}O_7H^+$),	84.05 ($C_4H_5ONH^+$),
201.18 ($C_{15}H_{20}H^+$),	331.32 ($C_{20}H_{42}O_3H^+$),	94.04 (X),
203.08 ($C_{11}H_{10}O_2N_2H^+$),	345.33 ($C_{21}H_{44}O_3H^+$),	104.04 ($C_7H_5NH^+$),
222.06 ($C_7H_{11}O_7NH^+$),	347.27 ($C_{26}H_{44}H^+$),	106.03 ($C_6H_3ONH^+$),
233.22 ($C_{17}H_{28}H^+$),	389.39 ($C_{27}H_{48}OH^+$),	106.07 ($C_7H_7NH^+$),
245.22 ($C_{18}H_{28}H^+$),	432.08 ($C_{16}H_{17}O_{13}NH^+$),	112.04 ($C_5H_5O_2NH^+$),
261.24 ($C_{15}H_{32}O_3H^+$),	438.42 ($^{13}CC_{31}H_{52}H^+$)	118.06 ($C_8H_7NH^+$)
273.24 ($C_{16}H_{32}O_3H^+$),		

ranging from 15 to 32 contributed the second biggest fraction (2 at city site, 1 at coastal and 5 at forest site). This is not surprising taking into account that the main constituents of crude oil, gas or exhaust of vehicles belong to the CH chemical class (e.g. benzene, 2-Methylpentane, n-Hexane, toluene) (Kawashima and Murakami, 2014). m/z 181.07 and m/z 203.08 ions were the same as ions detected in a Tunnel study of diesel vehicle emissions in Brazil (Oyama et al., 2015).

Fig. 8 shows that a negative correlation of $\delta^{13}C$ was not limited to individual ions. The mass fraction of all CH ions, also shows a negative correlation at low desorption temperatures. If the data measured at 150 °C and 200 °C are combined this yields a negative correlation with $r = -0.87$, $p = 8.34 \cdot 10^{-4}$ at the forest site and $r = -0.74$, $p = 7.5 \cdot 10^{-5}$ at the city site.

Biomass burning aerosol is usually enriched in ^{13}C with respect to the aerosol particles generated by fossil fuel combustion. Therefore, high values of $\delta^{13}C_{OC}$ can indicate an increased contribution of biomass burning to the respective carbon fraction. The positive slope of $\delta^{13}C$ vs. the mass fraction of any ion may be an indication that the origin of this ion is related to biomass burning
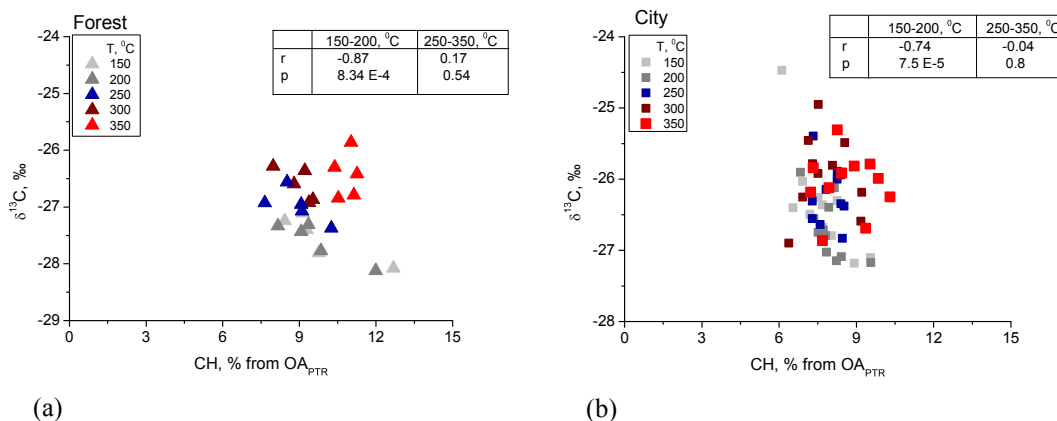
Fig. 8. The CH, % from all OA_{PTR} fraction via $\delta^{13}C_{OC}$ values at forest (a) and city (b) sites.

(BB). Therefore, we tentatively label these ions as "indicative of BB" in the remainder of the manuscript.

For example, a positive coefficient of correlation ($r = 0.75$) of $\delta^{13}C_{OC}$ with the mass fraction is observed for the ion with m/z = 42.034 ($C_2H_3NH^+$) ion at high desorption temperatures (300–350 °C). m/z = 42.034 ($C_2H_3NH^+$) can be attributed to acetonitrile (Holzinger et al., 1999), which is unlikely to be present in the aerosol directly due to its high vapour pressure. Thus, m/z = 42.034 is more likely a product of fragmentation of large organic compounds during thermal desorption. The positive correlation suggested that m/z = 42.034 (Fig. 9 (a)) is related to a source enriched in ^{13}C compared to the average ambient aerosol. In case of acetonitrile (m/z = 42.034), the association with biomass burning is well known.

12 other ions at the city site, 2 ions at the coastal site and 9 ions at the forest site showed a significant positive correlation with $\delta^{13}C_{OC}$ in the high temperature range, similar to $C_2H_3NH^+$. We therefore suggest that they might be indicative of biomass burning as well (Table 2). The majority of ions characterized as indicative of BB by this method (17 out of 23) contained nitrogen in their empirical formulas. A few previous studies (Karlsson et al., 2013; Schurman et al., 2015) demonstrated that nitrogen containing compounds made a significant contribution to biomass burning aerosol. However, some ions characterized as indicative of BB, for example CH_4OH^+ at the city site ($r = 0.53$; $p = 0.012$; Fig. 9 (b)), did not contain nitrogen.

Fig. 10 shows a scatter plot of the total mass fraction of all CHN ions analysed versus $\delta^{13}C$ at the forest site. The mass fraction of
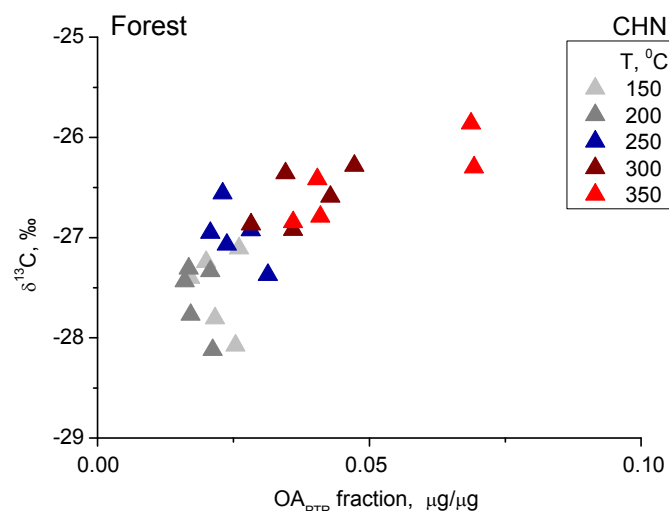

Fig. 10. Correlation of OA_{PTR} fraction via $\delta^{13}C_{OC}$ values of CHN ions desorbing at different temperatures at the forest site.

CHN was positively correlated with $\delta^{13}C$ ($r = 0.77$; $p = 0.009$) in the high temperature range (300–350 °C). Therefore, it is possible that organic nitrogen compounds are indicative of BB in Lithuanian wintertime. Theoretically it is possible that higher $\delta^{13}C$ values related to CHN ions indicate a marine source. However, the marine
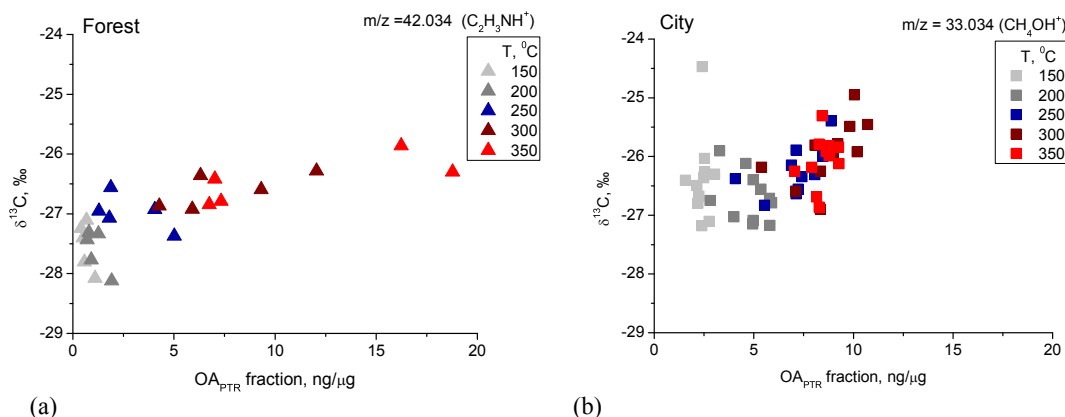

Fig. 9. OA_{PTR} fraction via $\delta^{13}C_{OC}$ values for individual ions as indicative of BB at forest (a) and city (b) sites.

source contribution to the fine mode particles was likely negligible both due to the distance to the nearest marine source (Vilnius city is 300 km from the Baltic Sea and about 1000 km from the Atlantic Ocean and the distance of the forest site location is 350 km from the Baltic Sea] as well as the magnitude of the marine source contribution to absolute OM concentrations observed in an urban and forest area.

A scatter plot of the O/C ratio, versus $\delta^{13}C_{OC}$ values at individual desorption temperatures is shown in Fig. 11 for city, coastal and forest sites. A positive correlation between O/C and $\delta^{13}C_{OC}$ at low desorption temperatures (150–250 °C) is determined at all three sites. At the city site the positive correlation is significant only at T = 150 °C (r = 0.88, p < 0.05). Surprisingly, there is a very clear negative correlation of O/C ratio with $\delta^{13}C_{OC}$ at the forest site for the highest desorption temperature of 350 °C (r = −0.99, p < 0.05). At this desorption temperature, 98% of the variation in $\delta^{13}C_{OC}$ can be explained by variations in the O/C ratio.

The reason for this anti-correlation is not entirely clear, but we propose a hypothesis related to chemical processing of the organic carbon. It is generally accepted that oxidative processing of primary emissions in the atmosphere gradually produces more refractory, highly oxidized organic aerosol (Crippa et al., 2013; Hallquist et al., 2009; Zhang et al., 2007). Therefore, we assume that on average the parent compounds are less refractory than the reaction products. At the same time, we expect that the chemical oxidation reactions are accompanied by isotopic fractionation. The fractionation leads to depletion in ^{13}C of the products and to the enrichment of the parent compounds in respect of the initial material.

The reaction products that remain in the particle phase will therefore be on the average more refractory and depleted in ^{13}C relative to the parent compounds. If oxidative processing is strong, the OC at low desorption temperatures should gradually become enriched in ^{13}C in respect of the initial OC. On the other hand, the OC at high desorption temperature, where reaction products accumulate, should gradually become depleted in ^{13}C with respect to the initial OC. If the O/C ratio is taken as an indicator of the extent of chemical processing, then δ^{13}C of the less refractory carbon should increase as O/C increases, resulting in a positive correlation. On the other hand, δ^{13}C of the more refractory section should decrease with the O/C ratio, resulting in a negative correlation.

4. Discussion

4.1. Evidence of oxidative processing at the forest site

The organic aerosol at the forest site was on average more refractory and contained a higher fraction of larger organic molecules than the aerosol at the city and coastal site. Moreover, the H/C ratios were negatively correlated with O/C ratios. Additionally, a distinct correlation pattern of $\delta^{13}C_{OC}$ with the O/C ratio was detected for high and low desorption temperature. This correlation pattern may be related to oxidative processing of the aerosol, even though this hypothesis is speculative. However, we observe this correlation pattern only at the forest site, the only site where other evidence of oxidative processing of the aerosol was observed. Together these observations strongly suggest that OA at the forest site was affected by oxidative processing in contrast to the OA at city and coastal site, which are much closer to direct sources.

The O/C and H/C data in this study compare well with observations of atmospheric oxidation state of the organic aerosol in numerous studies (Jimenez et al., 2009; Ng et al., 2011; Slowik et al., 2010; Vakkari et al., 2014). Slowik et al. (2010) showed a positive correlation of concentration of organic aerosol with increase of the ambient temperature. The monthly averaged temperature was −4 °C during our sample campaign and this could be a reason of the low (0.05 $\mu g/m^3$) monthly averaged OA_{PTR} at the forest site in

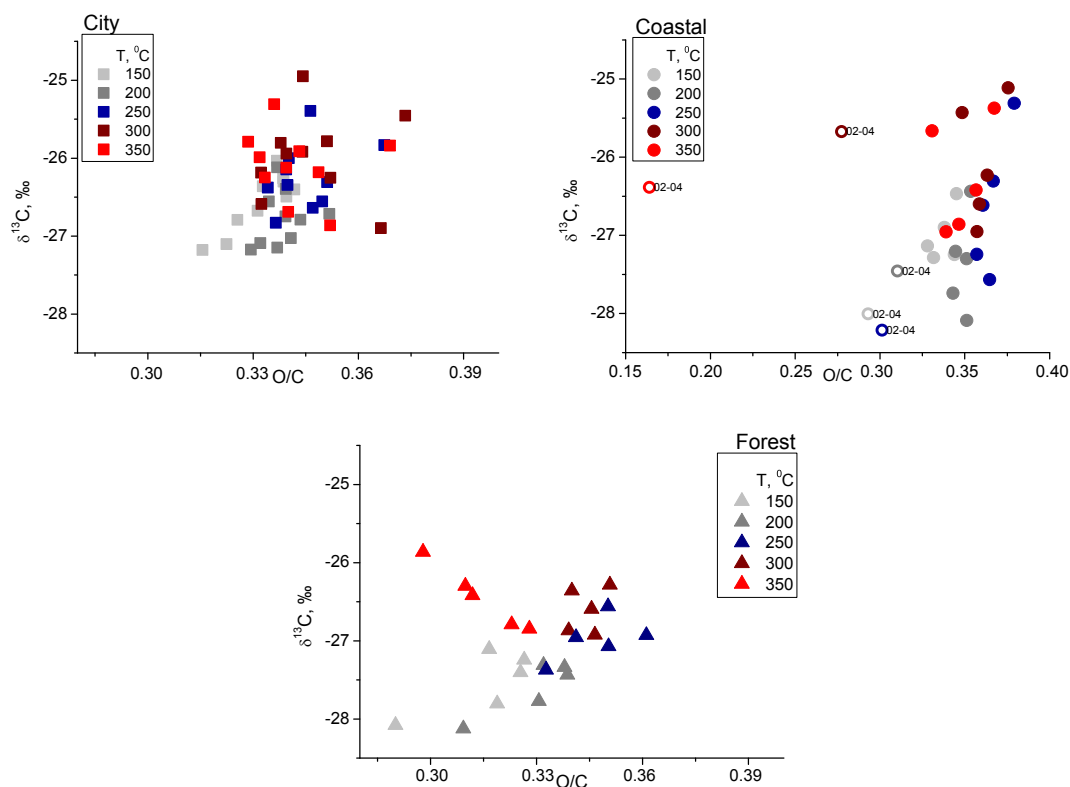**Fig. 11.** O/C via $\delta^{13}C_{OC}$ values at different T regime at city, coastal and forest sites (the monthly average of the data).

our study. Vakkari et al. (2014) reported that the lowest O/C ratios (0.37) of BB plumes correlated well with fresh OA. All these studies support our presumption that the variation of O/C ratios (0.31−0.36) measured in this study could be explained as a mix of different fresh and aged sources.

Some previous studies have used $\delta^{13}C$ isotope ratios to study the photochemical processing or aging of organic aerosol. Many of these studies have found enrichment in $\delta^{13}C$ for aged organic aerosol compared to recently emitted organic aerosol (Kirillova et al., 2013, 2014; Wang et al., 2010). The enrichment in $\delta^{13}C$ of the total organic carbon with increasing photochemical aging time is plausible. In oxidative processing a part of the depleted chemical reaction products partitions to the gas phase, which results in an enriched aerosol phase. In our observations we detect this enrichment mainly in the less refractory carbon fractions. Several other studies have focused on the $\delta^{13}C$ ratios of an individual "parent" compounds, such as oxalic acid that is degraded by photochemical processing. These have shown isotopic enrichment of the parent compound in the laboratory (if Fe^{2+} and Fe^{3+} iron was present as catalyst (Pavuluri and Kawamura, 2012)) and also under ambient conditions (Wang and Kawamura, 2006). Some elements of our hypothesis that relate the observed correlation pattern of $\delta^{13}C$ with O/C ratio to oxidative processing of the aerosol are therefore consistent with findings in the previous literature. Other elements, such as the accumulation of depleted reaction products in the more refractory OC, should be further investigated in controlled laboratory experiments.

4.2. Variations in $\delta^{13}C_{OC}$ related to individual ions detected by the PTR-MS

Considerable differences of $\delta^{13}C_{TC}$ and $\delta^{13}C_{OC}$ values between three sites have been observed. In Lithuania, carbonaceous aerosol from traffic emissions is depleted in ^{13}C with respect to aerosol from biomass burning emission by ~3‰. Therefore, observed variations in $\delta^{13}C_{OC}$ and $\delta^{13}C_{TC}$ can be caused by changes in the relative contribution of these two sources, such that OA enriched in ^{13}C compared to average conditions has a stronger contribution from biomass burning sources. However, the exact $\delta^{13}C_{TC}$ and $\delta^{13}C_{OC}$ values representative of regional biomass burning emissions are relatively difficult to quantify, because the proportions of biomass fuels used in Lithuania are not well established and $\delta^{13}C_{TC}$ in biomass burning emissions can be relatively variable, depending on fuel and burning conditions. Therefore we have not used $\delta^{13}C$ values for a quantitative source apportionment.

Instead, we demonstrated more qualitatively that variations in $\delta^{13}C_{OC}$ are in some cases correlated with the mass fraction of individual ions. In case of a positive correlation we assume that this ion is related to non-fossil sources and in case of a negative correlation it is related to fossil fuel combustion. This is an empirical association of a particular ion with a certain source, namely that the mass fraction of this ion in the OA increases with the source contribution, as traced by ^{13}C. The ions, identified by the 'top down' approach as indicative of a certain source in our study, are not tracers in the classical sense, which are unambiguously measured in a source profile, and fulfil other criteria, such as being unique to the source and chemically stable. On the other hand, this 'top down' approach may identify tracers that are missed by the classical approach because they may be secondary products that are nevertheless related to a particular source. This approach is very different from e.g., positive matrix factorisation analysis of aerosol mass spectra that allows identifying separate groups of organic aerosol (Zhang et al., 2011) and from tracer identification measurements that give straight access to tracers of specific sources (Claeys et al., 2004; Feng et al., 2013; Graham et al., 2004; Simoneit

et al., 1999). It gives more qualitative results and would be most useful in combination with one of the more established source apportionment methods.

In the 'top down' approach the ions can only be identified via their correlation with $\delta^{13}C_{OC}$ and often not be identified, if the $\delta^{13}C_{OC}$ is very variable, for example due to a number of unrelated sources, or sources that contribute differently to different particle sizes. At the city site a number of smaller sources, such as cooking, waste burning, or industrial sources (Crippa et al., 2013; Elser et al., 2016), could all influence the variation of $\delta^{13}C_{OC}$ and it is therefore more difficult to identify ions that are indicative of fossil fuel emission or biomass burning. On the contrary, the forest site is a remote place without any local anthropogenic pollution. Because of the low and potentially rather stable background OA concentrations at the forest site, $\delta^{13}C_{OC}$ can be strongly influenced by transport of pollution from fossil sources to the site and therefore the correlations of $\delta^{13}C_{OC}$ with individual ions are relatively strong and more ions are identified that could be indicative of BB or FF combustion sources. While the identification of particular ions as indicative of fossil fuel combustion or biomass burning is relatively speculative and subject to a number of assumptions, there is supporting evidence that strengthens this association.

- The ions that are identified as indicative of fossil fuel burning based on their correlation with $\delta^{13}C_{OC}$ are less oxidized than bulk OA.
- The suggested structures for a number of these ions contain relatively long alkane chains with some oxygen functional groups (e.g., m/z 261.24, m/z 273.24, m/z 287.27, m/z 289.28).
- m/z 345.33 ($C_{16}H_{32}O_3$) could be hydroxyhexadecanioc acid, and it has been found as the most abundant acid in a Tunnel study in France (El Haddad et al., 2009).
- m/z 331.32 ($C_{20}H_{42}O_3H+$), and m/z 345.33 ($C_{21}H_{44}O_3H+$) are likely based on C20 and C21 alkanes substituted with some oxygen functional groups. C20 and C21 were the most abundant alkanes found in the same Tunnel study and are especially prominent in diesel emissions (El Haddad et al., 2009 and references therein).
- m/z 181.07 and m/z 203.08 have very similar masses to ions found at high concentrations in diesel vehicle emissions in a Tunnel study in Brazil (Oyama et al., 2015).
- Not only individual ions, but also the mass fraction of all CH ions also shows a negative correlation with $\delta^{13}C_{OC}$. It is generally recognized that CH compounds or hydrocarbon-like OA fractions are strongly associated with fossil fuel combustion. This negative correlation is especially evident at low desorption temperatures, indicating that CH compounds in the more refractory organic material might have some other sources than fossil fuel combustion.

Biomass burning emissions generally have higher organic nitrogen content than fossil fuel emission; therefore the high abundance of N-containing compounds in the ions that are indicative of BB and the positive correlation of CHN ions with $\delta^{13}C_{OC}$ is credible.

5. Conclusions and outlook

The importance of the main sources of organic carbon and the effects of photochemical processing during wintertime on the chemical and isotopic composition were investigated using aerosol samples from three sites situated in Lithuania: the urban location of Vilnius, the coastal location of Preila and the forest location of Rugsteliskis. Detailed chemical composition and stable carbon isotope measurements provided insight into sources and properties of the organic aerosol fraction. The contribution of the broad

chemical classes (CH, CHO, CHN, CHON, X) to the total carbon was similar at all three sites. However, an analysis at different desorption temperatures revealed that aerosol particles from the remote forest site were more refractory and contained a larger fraction of heavy ions with m/z > 200. These two observations give an indication of photochemical processing during air mass transport to the forest site.

Two types of indicators of the main pollution sources were introduced using correlation between the mass fraction of individual compounds and $\delta^{13}C_{OC}$. Compounds, tentatively identified as indicative of BB, were characterized by positive correlation and high concentrations at the high desorption temperatures. Most of these organic compounds contained nitrogen. Additionally, the mass fraction of all CHN compounds was also positively correlated with $\delta^{13}C_{OC}$ at high desorption temperatures. Compounds indicative of FF were associated with a negative correlation with $\delta^{13}C_{OC}$ in the low (or all) temperature intervals. These compounds contained a number of heavy hydrocarbons and were on the average less oxidized than the bulk OC.

The investigation of the co-variation of O/C ratio and $\delta^{13}C_{OC}$ values at individual desorption temperatures revealed positive correlations at low desorption temperatures and negative (or no) correlations at high desorption temperatures at all three sites. We propose a hypothesis that this might be due to oxidative processing of the aerosol. The results of this study showed that carbon isotope analysis can potentially give insight into chemical processing of the carbonaceous aerosol. However, more research and laboratory experiments are necessary to test the hypothesis before a firm conclusion can be drawn.

Acknowledgements

References

Andreae, M., Talbot, R., Andreae, T., Harriss, R., 1988. Formic and acetic acid over the central Amazon region, Brazil: 1. Dry season. J. Geophys. Res. Atmos. 93, 1616–1624.

Andreae, M.O., Merlet, P., 2001. Emission of trace gases and aerosols from biomass burning. Glob. Biogeochem. Cycles 15, 955–966.

Asmi, A., Wiedensohler, A., Laj, P., Fjaeraa, A.-M., Sellegri, K., Birmili, W., Weingartner, E., Baltensperger, U., Zdimal, V., Zikova, N., 2011. Number size distributions and seasonality of submicron particles in Europe 2008–2009. Atmos. Chem. Phys. 11, 5505–5538.

Byčenkienė, S., Dudoitis, V., Ulevicius, V., 2014a. The use of trajectory cluster analysis to evaluate the long-range transport of black carbon aerosol in the South-Eastern baltic region. Adv. Meteorol 2014.

Byčenkienė, S., Plauškaitė, K., Dudoitis, V., Ulevicius, V., 2014b. Urban background levels of particle number concentration and sources in Vilnius, Lithuania. Atmos. Res. 143, 279–292.

Bovchaliuk, A., Milinevsky, G., Danylevsky, V., Goloub, P., Dubovik, O., Holdak, A., Ducos, F., Sosonkin, M., 2013. Variability of aerosol properties over Eastern Europe observed from ground and satellites in the period from 2003 to 2011. Atmos. Chem. Phys. 13, 6587–6602.

Bressi, M., Sciare, J., Ghersi, V., Mihalopoulos, N., Petit, J.-E., Nicolas, J., Moukhtar, S., Rosso, A., Féron, A., Bonnaire, N., 2014. Sources and geographical origins of fine aerosols in Paris (France). Atmos. Chem. Phys. 14, 8813–8839.

Cavalli, F., Viana, M., Yttri, K., Genberg, J., Putaud, J.-P., 2010. Toward a standardised thermal-optical protocol for measuring atmospheric organic and elemental carbon: the EUSAAR protocol. Atmos. Meas. Tech. 3, 79–89.

Ceburnis, D., Garbaras, A., Szidat, S., Rinaldi, M., Fahrni, S., Perron, N., Wacker, L., Leinert, S., Remeikis, V., Facchini, M., 2011. Quantification of the carbonaceous matter origin in submicron marine aerosol by 13 C and 14 C isotope analysis. Atmos. Chem. Phys. 11, 8593–8606.

Chen, Q., Heald, C.L., Jimenez, J.L., Canagaratna, M.R., Zhang, Q., He, L.Y., Huang, X.F., Campuzano-Jost, P., Palm, B.B., Poulain, L., 2015. Elemental composition of organic aerosol: the gap between ambient and laboratory measurements. Geophys. Res. Lett. 42.10, 4182–4189.

Chhabra, P., Ng, N., Canagaratna, M., Corrigan, A., Russell, L., Worsnop, D., Flagan, R.,

Seinfeld, J., 2011. Elemental composition and oxidation of chamber organic aerosol. Atmos. Chem. Phys. 11, 8827–8845.

Claeys, M., Graham, B., Vas, G., Wang, W., Vermeylen, R., Pashynska, V., Cafmeyer, J., Guyon, P., Andreae, M.O., Artaxo, P., 2004. Formation of secondary organic aerosols through photooxidation of isoprene. Science 303, 1173–1176.

Collier, S., Zhou, S., Kuwayama, T., Forestieri, S., Brady, J., Zhang, M., Kleeman, M., Cappa, C., Bertram, T., Zhang, Q., 2015. Organic PM emissions from vehicles: composition, O/C ratio, and dependence on PM. Conc. Aerosol Sci. Technol. 49, 86–97.

Crippa, M., DeCarlo, P., Slowik, J., Mohr, C., Heringa, M., Chirico, R., Poulain, L., Freutel, F., Sciare, J., Cozic, J., 2013. Wintertime aerosol chemical composition and source apportionment of the organic fraction in the metropolitan area of Paris. Atmos. Chem. Phys. 13, 961–981.

Deines, P., 1980. In: Fritz, P., Fontes, J. Ch (Eds.), Handbook of Environmental Isotope Geochemistry, vol. 1. Elsevier, New York, p. 329.

Dockery, D.W., Pope, C.A., Xu, X., Spengler, J.D., Ware, J.H., Fay, M.E., Ferris Jr., B.G., Speizer, F.E., 1993. An association between air pollution and mortality in six US cities. N. Engl. J. Med. 329, 1753–1759.

Dusek, U., Meusinger, C., Oyama, B., Ramon, W., de Wilde, P., Holzinger, R., Röckmann, T., 2013a. a thermal desorption system for measuring δ^{13} C ratios on organic aerosol. J. Aerosol Sci. 66, 72–82.

Dusek, U., Ten Brink, H., Meijer, H., Kos, G., Mrozek, D., Röckmann, T., Holzinger, R., Weijers, E., 2013b. The contribution of fossil sources to the organic aerosol in The Netherlands. Atmos. Environ. 74, 169–176.

El Haddad, I., Marchand, N., Dron, J., Temime-Roussel, B., Quivet, E., Wortham, H., Jaffrezo, J.L., Baduel, C., Voisin, D., Besombes, J.L., Gille, G., 2009. Comprehensive primary particulate organic characterization of vehicular exhaust emissions in France. Atmos. Environ. 43 (39), 6190–6198.

Elser, M., Bozzetti, C., El-Haddad, I., Maasikmets, M., Teinemaa, E., Richter, R., Wolf, R., Slowik, J.G., Baltensperger, U., Prévôt, A.S., 2016. Urban increments of gaseous and aerosol pollutants and their sources using mobile aerosol mass spectrometry measurements. Atmos. Chem. Phys. 16, 7117–7134.

Faiola, C., Wen, M., VanReken, T., 2015. Chemical characterization of biogenic secondary organic aerosol generated from plant emissions under baseline and stressed conditions: inter-and intra-species variability for six coniferous species. Atmos. Chem. Phys. 15, 3629–3646.

Feng, J., Li, M., Zhang, P., Gong, S., Zhong, M., Wu, M., Zheng, M., Chen, C., Wang, H., Lou, S., 2013. Investigation of the sources and seasonal variations of secondary organic aerosols in PM 2.5 in Shanghai with organic tracers. Atmos. Environ. 79, 614–622.

Fisseha, R., Spahn, H., Wegener, R., Hohaus, T., Brasse, G., Wissel, H., Tillmann, R., Wahner, A., Koppmann, R., Kiendler-Scharr, A., 2009. Stable carbon isotope composition of secondary organic aerosol from β-pinene oxidation. J. Geophys. Res. Atmos. 114 (1984–2012).

Fountoukis, C., Megaritis, A., Skyllakou, K., Charalampidis, P., Pilinis, C., Denier Van Der Gon, H., Crippa, M., Canonaco, F., Mohr, C., Prévôt, A., 2014. Organic aerosol concentration and composition over Europe: insights from comparison of regional model predictions with aerosol mass spectrometer factor analysis. Atmos. Chem. Phys. 14, 9061–9076.

Freney, E., Sellegri, K., Canonaco, F., Colomb, A., Borbon, A., Michoud, V., Doussin, J.-F., Crumeyrolle, S., Amarouche, N., Pichon, J.-M., 2014. Characterizing the impact of urban emissions on regional aerosol particles: airborne measurements during the MEGAPOLI experiment. Atmos. Chem. Phys. 14, 1397–1412.

Garbaras, A., Andriejauskiene, J., Bariseviciute, R., Remeikis, V., 2008. Tracing of atmospheric aerosol sources using stable carbon isotopes. Lith. J. Phys. 48, 259–264.

Garbaras, A., Jurgelionis, A., Rimkus, A., Nagurnas, S., Matijosius, J., Pukalskas, S., Remeikis, V., 2013. Study of Aerosol Particles 13C Values from Diesel Vehicles Exhaust. Isotopes 2013, Sopot, Poland, p. 77.

Garbaras, A., Masalaite, A., Garbariene, I., Ceburnis, D., Krugly, E., Remeikis, V., Puida, E., Kvietkus, K., Martuzevicius, D., 2015. Stable carbon fractionation in size-segregated aerosol particles produced by controlled biomass burning. J. Aerosol Sci. 79, 86–96.

Garbaras, A., Rimselyte, I., Kvietkus, K., Remeikis, V., 2009. delta13C values in size-segregated atmospheric carbonaceous aerosols at a rural site in Lithuania. Lith. J. Phys. 49, 229–236.

Garbariene, I., Šapolaitė, J., Garbaras, A., Ežerinskis, Ž., Pocevičius, M., Kriksčikas, L., Plukis, A., Remeikis, V., 2016. Origin identification of carbonaceous aerosol particles by carbon isotope ratio analysis. Aerosol Air Qual. Res. 16, 1356–1365.

Gelencsér, A., May, B., Simpson, D., Sánchez-Ochoa, A., Kasper-Giebl, A., Puxbaum, H., Caseiro, A., Pio, C., Legrand, M., 2007. Source apportionment of PM2. 5 organic aerosol over Europe: primary/secondary, natural/anthropogenic, and fossil/biogenic origin. J. Geophys. Res. Atmos. 112 (1984–2012).

Gensch, I., Kiendler-Scharr, A., Rudolph, J., 2014. Isotope ratio studies of atmospheric organic compounds: principles, methods, applications and potential. Int. J. mass Spectrom. 365, 206–221.

Górka, M., Jedrysek, M.-O., 2008. d 13 C of organic atmospheric dust deposited in Wrocław (SW Poland): critical remarks on the passive method. Geol. Q. 52, 115–126.

Graham, B., Falkovich, A.H., Rudich, Y., Maenhaut, W., Guyon, P., Andreae, M.O., 2004. Local and regional contributions to the atmospheric aerosol over Tel Aviv, Israel: a case study using elemental, ionic and organic tracers. Atmos. Environ. 38, 1593–1604.

Hallquist, M., Wenger, J., Baltensperger, U., Rudich, Y., Simpson, D., Claeys, M., Dommen, J., Donahue, N., George, C., Goldstein, A., 2009. The formation,

properties and impact of secondary organic aerosol: current and emerging issues. Atmos. Chem. Phys. 9, 5155—5236.

Holzinger, R., 2015. PTRwid: a new widget-tool for processing PTR-TOF-MS data. Atmos. Meas. Tech. Discuss. 8, 1629—1669.

Holzinger, R., Goldstein, A., Hayes, P., Jimenez, J., Timkovsky, J., 2013. Chemical evolution of organic aerosol in Los Angeles during the CalNex 2010 study. Atmos. Chem. Phys. 13, 10125—10141.

Holzinger, R., Kasper-Giebl, A., Staudinger, M., Schauer, G., Röckmann, T., 2010a. Analysis of the chemical composition of organic aerosol at the Mt. Sonnblick observatory using a novel high mass resolution thermal-desorption proton-transfer-reaction mass-spectrometer (hr-TD-PTR-MS). Atmos. Chem. Phys. 10, 10111—10128.

Holzinger, R., Millet, D., Williams, B., Lee, A., Kreisberg, N., Hering, S., Jimenez, J., Allan, J., Worsnop, D., Goldstein, A., 2007. Emission, oxidation, and secondary organic aerosol formation of volatile organic compounds as observed at Chebogue Point, Nova Scotia. J. Geophys. Res. Atmos. 112 (1984—2012).

Holzinger, R., Warneke, C., Hansel, A., Jordan, A., Lindinger, W., Scharffe, D.H., Schade, G., Crutzen, P.J., 1999. Biomass burning as a source of formaldehyde, acetaldehyde, methanol, acetone, acetonitrile, and hydrogen cyanide. Geophys. Res. Lett. 26, 1161—1164.

Holzinger, R., Williams, J., Herrmann, F., Lelieveld, J., Donahue, N., Röckmann, T., 2010b. Aerosol analysis using a Thermal-Desorption Proton-Transfer-Reaction Mass Spectrometer (TD-PTR-MS): a new approach to study processing of organic aerosols. Atmos. Chem. Phys. 10, 2257—2267.

Huffman, J., Docherty, K., Aiken, A., Cubison, M., Ulbrich, I., DeCarlo, P., Sueper, D., Jayne, J., Worsnop, D., Ziemann, P., 2009. Chemically-resolved aerosol volatility measurements from two megacity field studies. Atmos. Chem. Phys. 9, 7161—7182.

Jayne, J.T., Leard, D.C., Zhang, X., Davidovits, P., Smith, K.A., Kolb, C.E., Worsnop, D.R., 2000. Development of an aerosol mass spectrometer for size and composition analysis of submicron particles. Aerosol Sci. Technol. 33, 49—70.

Jimenez, J., Canagaratna, M., Donahue, N., Prevot, A., Zhang, Q., Kroll, J., DeCarlo, P., Allan, J., Coe, H., Ng, N., 2009. Evolution of organic aerosols in the atmosphere. Science 326, 1525—1529.

Karl, T., Christian, T.J., Yokelson, R.J., Artaxo, P., Hao, W.M., Guenther, A., 2007. The Tropical Forest and Fire Emissions Experiment: method evaluation of volatile organic compound emissions measured by PTR-MS, FTIR, and GC from tropical biomass burning. Atmos. Chem. Phys. 7, 5883—5897.

Karlsson, P.E., Ferm, M., Tømmervik, H., Hole, L.R., Karlsson, G.P., Ruoho-Airola, T., Aas, W., Hellsten, S., Akselsson, C., Mikkelsen, T.N., 2013. Biomass burning in eastern Europe during spring 2006 caused high deposition of ammonium in northern Fennoscandia. Environ. Pollut. 176, 71—79.

Kaufman, Y.J., Tanré, D., Boucher, O., 2002. A satellite view of aerosols in the climate system. Nature 419, 215—223.

Kawashima, H., Haneishi, Y., 2012. Effects of combustion emissions from the Eurasian continent in winter on seasonal δ 13 C of elemental carbon in aerosols in Japan. Atmos. Environ. 46, 568—579.

Kawashima, H., Murakami, M., 2014. Measurement of the stable carbon isotope ratio of atmospheric volatile organic compounds using chromatography, combustion, and isotope ratio mass spectrometry coupled with thermal desorption. Atmos. Environ. 89, 140—147.

Kirillova, E.N., Sheesley, R.J., Andersson, A., Gustafsson, O., 2010. Natural abundance 13C and 14C analysis of water-soluble organic carbon in atmospheric aerosols. Anal. Chem. 82, 7973—7978.

Kirillova, E.N., Andersson, A., Sheesley, R.J., Kruså, M., Praveen, P., Budhavant, K., Safai, P., Rao, P., Gustafsson, Ö., 2013. 13C-and 14C-based study of sources and atmospheric processing of water-soluble organic carbon (WSOC) in South Asian aerosols. J. Geophys. Res. Atmos. 118, 614—626.

Kirillova, E.N., Andersson, A., Tiwari, S., Srivastava, A.K., Bisht, D.S., Gustafsson, Ö., 2014. Water-soluble organic carbon aerosols during a full New Delhi winter: isotope-based source apportionment and optical properties. J. Geophys. Res. Atmos. 119, 3476—3485.

Kourtchev, I., Fuller, S., Aalto, J., Ruuskanen, T.M., McLeod, M.W., Maenhaut, W., Jones, R., Kulmala, M., Kalberer, M., 2013. Molecular composition of boreal forest aerosol from Hyytiala, Finland, using ultrahigh resolution mass spectrometry. Environ. Sci. Technol. 47, 4069—4079.

Kroll, J.H., Seinfeld, J.H., 2008. Chemistry of secondary organic aerosol: formation and evolution of low-volatility organics in the atmosphere. Atmos. Environ. 42, 3593—3624.

Kvietkus, K., Šakalys, J., Rimšelytė, I., Ovadnevaitė, J., Remeikis, V., Špakauskas, V., 2011. Characterization of aerosol sources at urban and background sites in Lithuania. Lith. J. Phys. 51.

Laj, P., Klausen, J., Bilde, M., Plass-Duelmer, C., Pappalardo, G., Clerbaux, C., Baltensperger, U., Hjorth, J., Simpson, D., Reimann, S., 2009. Measuring atmospheric composition change. Atmos. Environ. 43, 5351—5414.

Lewis, A., Evans, M., Hopkins, J., Punjabi, S., Read, K., Purvis, R., Andrews, S., Moller, S., Carpenter, L., Lee, J., 2013. The influence of biomass burning on the global distribution of selected non-methane organic compounds. Atmos. Chem. Phys. 13, 851—867.

Masalaite, A., Garbaras, A., Remeikis, V., 2012. Stable isotopes in environmental investigations. Lith. J. Phys. 52, 261—268.

Masalaite, A., Remeikis, V., Garbaras, A., Dudoitis, V., Ulevicius, V., Ceburnis, D., 2015. Elucidating carbonaceous aerosol sources by the stable carbon δ13CTC ratio in size-segregated particles. Atmos. Res. 158—159, 1—12.

Meinorė, E., Šakalys, J., Kvietkus, K., 2015. Chemical composition, concentration and

source apportionment of atmospheric submicron aerosol particles at urban and background sites. Lith. J. Phys. 54.

Meusinger, C., Dusek, U., King, S., Holzinger, R., Rosenørn, T., Sperlich, P., Jiulien, M.S., Remaud, G., Bilde, M., Röckmann, T.S., Johnson, M., 2016. Chemical and isotopic composition of secondary organic aerosol generated by alfa-pinene ozonolysis. Atmos. Chem. Phys. Discuss. (submitted).

Milukaite, A., Kvietkus, K., Rimselyte, I., 2007. Organic and elemental carbon in crystal aerosol of the Baltic Sea. Lith. J. Phys. 47, 203—210.

Monks, P., Granier, C., Fuzzi, S., Stohl, A., Williams, M., Akimoto, H., Amann, M., Baklanov, A., Baltensperger, U., Bey, I., 2009. Atmospheric composition change—global and regional air quality. Atmos. Environ. 43, 5268—5350.

Nel, A., 2005. Air pollution-related illness: effects of particles. Science 308, 804—806.

Ng, N., Canagaratna, M., Jimenez, J., Chhabra, P., Seinfeld, J., Worsnop, D., 2011. Changes in organic aerosol composition with aging inferred from aerosol mass spectra. Atmos. Chem. Phys. 11, 6465—6474.

Oyama, B., Andrade, M., Herckes, P., Dusek, U., Röckmann, T., Holzinger, R., 2015. Vehicular emissions of organic particulate matter in Sao Paulo, Brazil. Atmos. Chem. Phys. Discuss. 15, 33755—33788.

Ovadnevaitė, J., Kvietkus, K., Maršalka, A., 2006. 2002 summer fires in Lithuania: impact on the Vilnius city air quality and the inhabitants health. Sci. Total Environ. 356, 11—21.

Ovadnevaitė, J., Kvietkus, K., Šakalys, J., 2007. Evaluation of the impact of long-range transport and aerosol concentration temporal variations at the eastern coast of the Baltic Sea. Environ. Monit. Assess. 132, 365—375.

Pavuluri, C.M., Kawamura, K., 2012. Evidence for 13-carbon enrichment in oxalic acid via iron catalyzed photolysis in aqueous phase. Geophys. Res. Lett. 39.

Peterson, M.R., Richards, M.H., 2002. Thermal-optical-transmittance Analysis for Organic, Elemental, Carbonate, Total Carbon, and OCX2 in PM2. 5 by the EPA/ NIOSH Method, Proceedings. In: Symposium on Air Quality Measurement Methods and Technology-2002. Air & Waste Management Association, Pittsburgh, PA, 83—81.

Pope, C.A., Dockery, D.W., 2006. Health effects of fine particulate air pollution: lines that connect. J. air & waste Manag. Assoc. 56, 709—742.

Presto, A., Gordon, T., Robinson, A., 2014. Primary to secondary organic aerosol: evolution of organic emissions from mobile combustion sources. Atmos. Chem. Phys. 14, 5015—5036.

Putaud, J.-P., Raes, F., Van Dingenen, R., Brüggemann, E., Facchini, M.-C., Decesari, S., Fuzzi, S., Gehrig, R., Hüglin, C., Laj, P., 2004. A European aerosol phenomenology—2: chemical characteristics of particulate matter at kerbside, urban, rural and background sites in Europe. Atmos. Environ. 38, 2579—2595.

Putaud, J.-P., Van Dingenen, R., Alastuey, A., Bauer, H., Birmili, W., Cyrys, J., Flentje, H., Fuzzi, S., Gehrig, R., Hansson, H.-C., 2010. A European aerosol phenomenology—3: physical and chemical characteristics of particulate matter from 60 rural, urban, and kerbside sites across Europe. Atmos. Environ. 44, 1308—1320.

Röckmann, T., Kaiser, J., Brenninkmeijer, C.A., Brand, W.A., 2003. Gas chromatography/isotope-ratio mass spectrometry method for high-precision position-dependent 15N and 18O measurements of atmospheric nitrous oxide. Rapid Commun. mass Spectrom. 17, 1897—1908.

Saccon, M., Kornilova, A., Huang, L., Moukhtar, S., Rudolph, J., 2015. Stable carbon isotope ratios of ambient secondary organic aerosols in Toronto. Atmos. Chem. Phys. 15, 10825—10838.

Schurman, M.I., Lee, T., Desyaterik, Y., Schichtel, B.A., Kreidenweis, S.M., Collett Jr., J.L., 2015. Transport, biomass burning, and in-situ formation contribute to fine particle concentrations at a remote site near Grand Teton National Park. Atmos. Environ. 112, 257—268.

Simoneit, B.R., Schauer, J.J., Nolte, C., Oros, D.R., Elias, V.O., Fraser, M., Rogge, W., Cass, G.R., 1999. Levoglucosan, a tracer for cellulose in biomass burning and atmospheric particles. Atmos. Environ. 33, 173—182.

Slowik, J., Stroud, C., Bottenheim, J., Brickell, P., Chang, R.-W., Liggio, J., Makar, P., Martin, R., Moran, M., Shantz, N., 2010. Characterization of a large biogenic secondary organic aerosol event from eastern Canadian forests. Atmos. Chem. Phys. 10, 2825—2845.

Stein, A.F., Draxler, R.R., Rolph, G.D., Stunder, B.J.B., Cohen, M.D., Ngan, F., 2015. NOAA's HYSPLIT atmospheric transport and dispersion modeling system. Bull. Am. Meteorol. Soc. 96, 2059—2077. http://dx.doi.org/10.1175/BAMS-D-14-00110.1.

Stubbins, A., Hood, E., Raymond, P.A., Aiken, G.R., Sleighter, R.L., Hernes, P.J., Butman, D., Hatcher, P.G., Striegl, R.G., Schuster, P., 2012. Anthropogenic aerosols as a source of ancient dissolved organic matter in glaciers. Nat. Geosci. 5, 198—201.

Takegawa, N., Miyazaki, Y., Kondo, Y., Komazaki, Y., Miyakawa, T., Jimenez, J., Jayne, J., Worsnop, D., Allan, J., Weber, R., 2005. Characterization of an aerodyne aerosol mass spectrometer (AMS): intercomparison with other aerosol instruments. Aerosol Sci. Technol. 39, 760—770.

Timkovsky, J., Dusek, U., Henzing, J.S., Kuipers, T.L., Röckmann, T., Holzinger, R., 2015. Offline thermal-desorption proton-transfer-reaction mass spectrometry to study composition of organic aerosol. J. Aerosol Sci. 79, 1—14.

Ulevicius, V., Byčenkienė, S., Bozzetti, C., Vlachou, A., Plauškaitė, K., Mordas, G., Dudoitis, V., Abbaszade, G., Remeikis, V., Garbaras, A., Masalaite, A., Blees, J., Fröhlich, R., Dällenbach, K., Canonaco, F., Slowik, J., Dommen, J., Zimmermann, R., Schnelle-Kreis, J., Salazar, G., Agrios, K., Szidat, S., El Haddad, I., Prévôt, A., 2016. Fossil and non-fossil source contributions to atmospheric carbonaceous aerosols during extreme spring grassland fires in Eastern Europe.

Atmos. Chem. Phys. 16, 5513—5529.

Ulevicius, V., Byčenkienė, S., Remeikis, V., Garbaras, A., Kecorius, S., Andriejauskienė, J., Jasinevičienė, D., Mocnik, G., 2010. Characterization of pollution events in the East Baltic region affected by regional biomass fire emissions. Atmos. Res. 98, 190—200.

Vakkari, V., Kerminen, V.M., Beukes, J.P., Tiitta, P., Zyl, P.G., Josipovic, M., Venter, A.D., Jaars, K., Worsnop, D.R., Kulmala, M., 2014. Rapid changes in biomass burning aerosols by atmospheric oxidation. Geophys. Res. Lett. 41, 2644—2651.

Wang, G., Xie, M., Hu, S., Gao, S., Tachibana, E., Kawamura, K., 2010. Dicarboxylic acids, metals and isotopic compositions of C and N in atmospheric aerosols from inland China: implications for dust and coal burning emission and secondary aerosol formation. Atmos. Chem. Phys. 10, 6087—6096.

Wang, H., Kawamura, K., 2006. Stable carbon isotopic composition of low-molecular-weight dicarboxylic acids and ketoacids in remote marine aerosols. J. Geophys. Res. Atmos. 111.

Weijers, E., Schaap, M., 2013. Anthropogenic and Natural Constituents in PM10 at Urban and Rural Sites in North-Western Europe: Concentrations, Chemical Composition and Sources, Urban Air Quality in Europe. Springer, pp. 239—258.

Widory, D., 2006. Combustibles, fuels and their combustion products: a view through carbon isotopes. Combust. Theory Model. 10, 831—841.

Widory, D., Roy, S., Le Moullec, Y., Goupil, G., Cocherie, A., Guerrot, C., 2004. The origin of atmospheric particles in Paris: a view through carbon and lead isotopes. Atmos. Environ. 38, 953—961.

Zhang, Y., Tang, L., Wang, Z., Yu, H., Sun, Y., Liu, D., Qin, W., Canonaco, F., Prévôt, A., Zhang, H., 2015. Insights into characteristics, sources, and evolution of submicron aerosols during harvest seasons in the Yangtze River delta region, China. Atmos. Chem. Phys. 15, 1331—1349.

Zhang, Q., Jimenez, J., Canagaratna, M., Allan, J., Coe, H., Ulbrich, I., Alfarra, M., Takami, A., Middlebrook, A., Sun, Y., 2007. Ubiquity and dominance of oxygenated species in organic aerosols in anthropogenically-influenced Northern Hemisphere midlatitudes. Geophys. Res. Lett. 34.

Zhang, Q., Jimenez, J.L., Canagaratna, M.R., Ulbrich, I.M., Ng, N.L., Worsnop, D.R., Sun, Y., 2011. Understanding atmospheric organic aerosols via factor analysis of aerosol mass spectrometry: a review. Anal. Bioanal. Chem. 401, 3045—3067.